https://doi.org/10.33271/nvngu/2026-4/077

D. V. Hryshchak[1],
orcid.org/0009-0009-8428-6520,
V. Z. Gristchak[*2],
orcid.org/0000-0001-8685-3191,
N. M. Dyachenko[3],
orcid.org/0000-0001-5284-4502,
V. O. Kuprikov[3],
orcid.org/0009-0008-3221-582X

1 – Pivdenne State Design Office named after M. K. Yangel, Dnipro, Ukraine
2 – Dnipro University of Technology, Dnipro, Ukraine
3 – Zaporizhzhia National University, Zaporizhzhia, Ukraine
* Corresponding author e-mail: HRYSHCHAK.V.Z@mnu.one

STABILITY AND BIFURCATIONS OF ECCENTRICALLY REINFORCED COMPOUND SHELL STRUCTURES BY MEANS OF COMPUTER ALGEBRA

Purpose. To develop an analytical-numerical approach and algorithms for applying a computer algebra system (CAS) to analyze the influence of the arrangement of reinforcing load-carrying elements on the stability of compound orthogonally stiffened shell structures under combined external loading. Achieving this objective involves deriving governing stability equations and developing algorithms for studying the dependence of critical loads on geometric and stiffness parameters of compartments, the arrangement of reinforcing structural elements, and the character of external loading

Methodology. A methodology for deriving the governing equations using the Maple system is proposed, along with an algorithm for numerical solution of the stability problem by the finite-difference method with computer visualization of bifurcation modes for the compartments and the compound shell system.

Findings. Based on computer algebra systems, an approach to solving the stability problem of a compound stiffened "cone–cylinder" shell system under combined external loading taking into account specific stiffness characteristics of the compartments is proposed. Algorithms are proposed for studying the influence of eccentricity of the reinforcing system, discrete arrangement of ring stiffeners, and visualization of the investigated processes with determination of characteristic bifurcation modes and construction of boundary curves separating the stability domain of the investigated structure under dominant external pressure.

Originality. The influence of eccentricity of reinforcing load-carrying elements relative to the midsurface of a compound shell structure under two-parameter loading by axial compressive forces and external pressure is established. Specific features of the influence of stiffness characteristics of the reinforcing system are identified based on the proposed algorithm for automated derivation of governing differential equations using computer algebra systems. Numerical results for critical loads of a "cone-cylinder" type system are presented.

Practical value. The conducted analysis makes it possible to identify the influence of the arrangement and stiffness characteristics of reinforcing load-carrying elements on the load-bearing capacity of compound "cone–cylinder" shell systems. The interaction of local and global bifurcation modes under combined loading is taken into account. The application of computer algebra systems enables the construction of boundary curves separating the stability region of the investigated system depending on the arrangement and configuration of stiffening ribs. The obtained results enable the design of structures that are rational with respect to the critical state.

Keywords: *computer algebra, compound shell, stiffening elements, eccentricity, stability equations, bifurcation modes*

Received: 03 February 2026
Accepted: 26 June 2026
Available online: 27 August 2026

Introduction. It is well known that compound thin-walled shell systems are widely used in civil engineering, aviation and aerospace engineering, chemical engineering, and other industries. This is especially true for structures operating under extreme conditions of combined external loading, where the combination of low weight with high stability and reliability is essential.

Effective ways to increase load-bearing capacity while minimizing material consumption include the use of reinforced shells of rotation with orthogonally arranged stiffeners or waffle-type load-bearing frameworks [1, 2]. These design solutions include systems with discretely spaced ring stiffeners [3, 4], sandwich shells [5, 6], shell sections made of composite materials [7, 8], and compound shell systems with nonzero Gaussian curvature of the midsurface [1, 9].

In studies devoted to the elastic stability of reinforced shell structures, orthotropic models with reduced stiffness of the reinforcing system are typically proposed [10, 11], as well as models that account for the discrete arrangement of load-bearing elements [6, 11]. However, analytical derivation of stability equations, especially for heterogeneous compound shell systems, is a technically cumbersome procedure.

Modern approaches in the analysis and design of shell-type structures are largely focused on the use of software packages implementing the finite element and finite difference analysis [5, 12]. At the same time, computer algebra systems (CAS) effectively complement modern computer-aided design (CAD) systems. They enable automation of analytical transformations and algorithmize for determining critical loads. In addition,

© Hryshchak D. V., Gristchak V. Z., Dyachenko N. M., Kuprikov V. O., 2026

CAS provide computer visualization of the processes under investigation. In stability problems of thin-walled systems, an important aspect is the analysis of bifurcation modes depending on the nature of critical external loading. This aspect further makes CAS a powerful tool for analysis of rational structural designs in terms of local and global buckling under combined loading [13, 14].

The application of computer algebra systems (CAS), as demonstrated in studies, makes it possible, particularly with the Maple system, to implement automated generation and derivation of governing stability equations for compound heterogeneous shell systems. Further transformation of the obtained equations and their numerical solution with graphical representation of results allows identification of new physical effects and prediction of load-carrying capacity of the investigated systems.

Literature review. A review of the current state of research on the stability of compound reinforced shell structures indicates that existing studies mainly focus on cylindrical [15, 16], conical [17], and compound "cone–cylinder" shell systems [12, 18]. The studies employ analytical and analytical-numerical approaches, including analysis of the influence of the sign of the midsurface curvature [8, 19] and initial imperfections [12, 20]. The influence of reinforcement layouts [17, 18], parameters of stiffening ribs [21, 22], and eccentricity of reinforcing load-carrying elements [4, 11] on critical loads of compartments and bifurcation modes is also investigated.

It is worth noting that numerical methods based on CAD systems, particularly ANSYS, ABAQUS, and other software packages, have significantly advanced stability analysis of modern structures, enabling 3D load-carrying capacity analysis of shell systems using specialized computational modules [2, 15]. The role of computer visualization of post-buckling deformation modes is also increasing, making it possible to trace the deformation process of structures under external loading [13, 14]. In some cases, such visualization reduces the need for physical experimental studies and serves as a basis for rational structural design from the standpoint of stability.

Recently, significant attention has been given to the study of the influence of multi-parameter external loading on the critical state of shell structures, since each parameter may lead to buckling. An important aspect is determining the boundary surface that limits the stability region depending on combinations of loading parameters and geometric and stiffness characteristics of the investigated systems [6, 13].

Unsolved aspects of the problem. Based on the analysis of existing approaches to the study of shell stability, the following unresolved issues can be identified:

- development of an algorithm for applying CAS to the analytical derivation of stability equations for elastic compound shell structure of the "cone–cylinder" type reinforced with an orthogonal stiffening system;

- consideration of the eccentricity sign of reinforcing load-carrying elements and discrete arrangement of transverse reinforcement (ring stiffeners), including their out-of-plane stiffness relative to the initial curvature;

- analysis of the effect of combined loading by external pressure and axial forces on a compound heterogeneous shell system;

- development of an algorithm for visualization of bifurcation modes in the presence of axial forces under dominant external pressure;

- design of rational compound shell structures based on equal stability of compartments and spans with respect to local and global bifurcation modes.

Purpose: development of an analytical-numerical approach for solving stability problems of compound heterogeneous shell structures of the "cone–cylinder" type; analysis of bifurcation states taking into account local and global modes; influence of stiffening ribs eccentricity relative to the midsurface and discrete arrangement of intermediate ring stiffeners; development of algorithms for numerical analysis, computer visualization of bifurcation modes, and construction of boundary curves defining the stability region under combined loading using Maple.

Problem formulation. A linear axisymmetric problem of elastic stability of a compound shell structure of the "cone-cylinder" type (Fig. 1) is considered. The structure is reinforced by densely arranged longitudinal and discretely spaced ring stiffening, taking into account the eccentricity of the reinforcing load-carrying elements (Figs. 1, *a*–*d*), as well as by connecting ring stiffeners (Fig. 1, *e*). The structure is subjected to combined loading capable of causing buckling, namely external pressure q and an axial compressive or tensile force T. The reinforcing system is modeled using an orthotropic scheme [10, 23] with discrete arrangement of intermediate and connecting ring stiffeners.

Figs. 1, *a*–*d* illustrate geometric schemes of stiffening ribs of the shell; the dashed line indicates the midsurface. Cross-sections of the shell with ring stiffening ribs (ring stiffeners) under one-sided and two-sided reinforcement are shown in Figs. 1, *a*, *c*, respectively, while those with longitudinal stiffening ribs (stringers) are shown in Figs. 1, *b*, *d*. In the case of two-sided reinforcement, the ribs are arranged symmetrically with respect to the midsurface of the shell.

Ring stiffeners, arranged transversely to the shell axis and uniformly along the generatrix, are characterized by height δ_2^p, thickness b_2, and spacing t_2 between the axes of adjacent ribs. Longitudinal ribs are oriented along the shell generatrix and are defined by height δ_1^p, thickness b_1, and transverse spacing t_1, which is equal to the arc length between the intersection points of their axes with the midsurface. All rib heights are measured from the inner or outer surface of the shell of thickness h, to which they are attached.

The coordinate system of the midsurface is defined as follows: for both sections, the axis of revolution is denoted by Oz; the coordinate along the generatrix of the cylinder or cone is $\overline{s}$ for the cylindrical segment and s for the conical segment; the ring coordinate of the cylinder is y, while for the cone the angular coordinate in the plane of its parallel is φ; at the base, α, l_0 and l_1 are the distances along the generatrix to the smaller and larger bases of the truncated conical shell; L and R are the generatrix length and the radius of the cylinder, respectively.

Following [1], a buckling mode dominated by variations of the stress-strain state in the circumferential direction is considered. This allows the use of the semi-

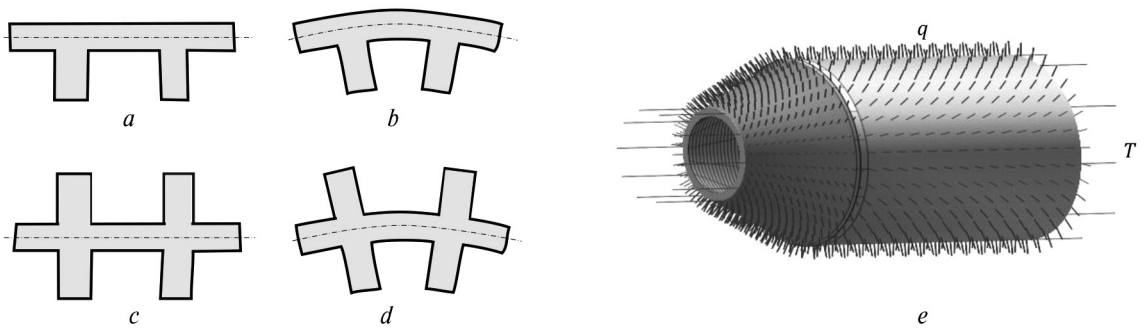

Fig. 1. Scheme of the reinforced compound shell structure "cone-cylinder"

membrane theory of thin elastic shells, provided that the wave number in the transverse direction of the midsurface at buckling satisfies the inequality $n^2 \gg 1$.

Algorithm for deriving the governing system of differential stability equations based on the Maple system. The following notations are introduced: N_1, N_2, T_{12}, T_{21} are the normal and shear forces per unit arc length; Q_1, Q_2 are the transverse shear forces in sections along the coordinate axes; M_1, M, H_{12}, H_{21} are the bending and twisting moments; A_1, A_2, R_1, R_2 are the parameters of lengths and curvatures of the midsurface.

The forces N_1, N_2 and moments M_1, M_2 in the case of two-sided reinforcement by ribs are expressed in terms of the normal strains ε_1, ε_2, and curvature variations κ_1, κ_2 by the formulas [24]

$$\begin{aligned} N_i &= \frac{E}{1-\nu^2}\int\limits_{-\frac{h}{2}}^{\frac{h}{2}} (\varepsilon_i + \nu\varepsilon_i + z(\kappa_i + \nu\kappa_j))dz + \\ &+ E\frac{b_i}{t_i}\left(\int\limits_{-\frac{h}{2}-\delta_i^p}^{\frac{h}{2}} (\varepsilon_i + z\kappa_i)dz + \int\limits_{-\frac{h}{2}}^{\frac{h}{2}+\delta_i^p} (\varepsilon_i + z\kappa_i)dz\right); \\ M_i &= \frac{E}{1-\nu^2}\int\limits_{-\frac{h}{2}}^{\frac{h}{2}} (\varepsilon_i + \nu\varepsilon_j + z(\kappa_i + \nu\kappa_j))zdz + \\ &+ E\frac{b_i}{t_i}\left(\int\limits_{-\frac{h}{2}-\delta_i^p}^{\frac{h}{2}} (\varepsilon_i + z\kappa_i)zdz + \int\limits_{-\frac{h}{2}}^{\frac{h}{2}+\delta_i^p} (\varepsilon_i + z\kappa_i)zdz\right), \end{aligned} \quad (1)$$

where E and ν are Young's modulus and Poisson's ratio of the shell material; the index i takes values $i = 1, 2$, and $j = 1$ for $i = 2$, and $j = 2$ for $i = 1$.

The second integrals in (1) correspond to internal ribs, and the third ones to external ribs. This allows accounting for the influence of eccentricity of reinforcement by representing the forces and bending moments in the midsurface cross-section in the form

$$\begin{aligned} N_i &= \frac{Eh}{1-\nu^2}(\omega_i\varepsilon_i + \nu\varepsilon_j) + Rh^2\lambda_i\kappa_i; \\ M_i &= \frac{Eh^3}{1-\nu^2}(i_i\kappa_i + \nu\kappa_j) + Rh^2\lambda_i\varepsilon_i, \end{aligned} \quad (2)$$

where the moments of inertia I_i^p of half of the rib cross-section with respect to the axes lying in the midsurface, as well as the auxiliary ribbing parameters i_i, ω_i, λ_i, are calculated by the formulas ($i = 1,2$)

$$i_i = 1 + C_1 \cdot \frac{12(1-\nu^2)I_i^p}{t_i h^3}; \quad \omega_i = 1 + C_1 \cdot \frac{b_i\delta_i^p(1-\nu^2)}{t_i h};$$

$$I_i^p = \frac{1}{12}b_i(\delta_i^p)^3 + \frac{1}{4}b_i\delta_i^p(h+\delta_i^p)^2;$$

$$\lambda_i = C_2 \cdot \frac{b_i}{t_i h^2}\delta_i^p(h+\delta_i^p).$$

Here, $C_1 = 1$ in the case of one-sided reinforcement and $C_1 = 2$ for two-sided reinforcement; $C_2 = \frac{1}{2}$ for shells reinforced with external ribs, $C_2 = -\frac{1}{2}$ for internal ribs, and $C_2 = 0$ for two-sided reinforcement. It should be noted that the obtained formulas are consistent with the results of [10].

The derivation of the governing differential stability equations for shell segments reinforced with symmetrically arranged two-sided ribs using the Maple system is reduced to the following steps. At the first stage, a scheme of reinforcement by ring and longitudinal stiffening ribs, symmetrically arranged with respect to the midsurface, is considered.

Step 1. The equations of the general shell theory [24], required for deriving the governing equations, are introduced. The coordinates ξ and η are defined to represent the system of equilibrium equations of the shell segments in projections onto the tangents to the coordinate lines and the normal direction

$$\begin{aligned} &\frac{\partial}{\partial\xi}(A_2N_1) + \frac{\partial}{\partial\eta}(A_2T_{21}) - N_2\frac{\partial A_2}{\partial\xi} + \\ &+ T_{12}\frac{\partial A_1}{\partial\eta} - Q_1\frac{A_1A_2}{R_1} = 0; \end{aligned} \quad (3)$$

$$\begin{aligned} &\frac{\partial}{\partial\eta}\left(A_1N_2\right) + \frac{\partial}{\partial\xi}\left(A_2T_{21}\right) - N_2\frac{\partial A_1}{\partial\eta} + \\ &+ T_{12}\frac{\partial A_2}{\partial\xi} - Q_2\frac{A_1A_2}{R_2} = 0; \end{aligned} \quad (4)$$

$$\frac{\partial}{\partial\xi}(A_1Q_1) + \frac{\partial}{\partial\eta}(A_2Q_2) + N_1\frac{A_1A_2}{R_1} + N_2\frac{A_1A_2}{R_2} + gA_1A_2 = 0. \quad (5)$$

Step 2. The equations for bending moments and forces with respect to the Oz axis are written in the form

$$\frac{\partial}{\partial\xi}(A_2M_1) + \frac{\partial}{\partial\eta}(A_1H_{21}) - M_2\frac{\partial A_2}{\partial\xi} + H_{12}\frac{\partial A_1}{\partial\eta} - Q_1A_1A_2 = 0; \quad (6)$$

$$\frac{\partial}{\partial\eta}(A_1M_2)+\frac{\partial}{\partial\xi}(A_2H_{21})-M_1\frac{\partial A_1}{\partial\eta}+H_{12}\frac{\partial A_2}{\partial\xi}-Q_2A_1A_2=0; \quad (7)$$

$$T_{12}-T_{21}-\frac{H_{12}}{R_1}+\frac{H_{21}}{R_2}=0. \quad (8)$$

If one assumes that if one sets $T_{12} = T_{21} = T_h$ and $H_{12} = H_{21} = H_h$, then for $R_1 \neq R_2$ equation (8) is not exactly satisfied; however, the resulting error is of the same order as that inherent in other equations of the classical theory of thin elastic shells [24].

Step 3. The compatibility equations for the strains ε_1, ε_2, ε_{12}

$$\frac{1}{A_1A_2}\left\{\frac{\partial}{\partial\xi}\frac{1}{A_1}\left(A_2\frac{\partial\varepsilon_2}{\partial\xi}+\frac{\partial A_2}{\partial\xi}(\varepsilon_2-\varepsilon_1)-\frac{A_1}{2}\frac{\partial\varepsilon_{12}}{\partial\eta}-\frac{\partial A_1}{\partial\eta}\varepsilon_{12}\right)+\right.$$
$$\left.+\frac{\partial}{\partial\eta}\frac{1}{A_2}\left(A_1\frac{\partial\varepsilon_1}{\partial\eta}+\frac{\partial A_1}{\partial\eta}(\varepsilon_1-\varepsilon_2)-\frac{A_2}{2}\frac{\partial\varepsilon_{12}}{\partial\xi}-\frac{\partial A_2}{\partial\xi}\varepsilon_{12}\right)\right\}- \quad (9)$$
$$-\frac{\kappa_1}{R_2}-\frac{\kappa_2}{R_1}=0.$$

Step 4. The function g of the fictitious transverse load is expressed in terms of the force distribution functions N_{10}, N_{20} in the basic pre-buckling membrane state

$$g=-(N_{10}\kappa_1+N_{20}\kappa_2), \quad (10)$$

where the curvatures are expressed through the deflection function w in the form

$$\kappa_1=-\frac{1}{A_1}\frac{\partial}{\partial\xi}\left(\frac{1}{A_1}\frac{\partial w}{\partial\xi}\right)-\frac{1}{(A_2)^2A_1}\frac{\partial A_1}{\partial\eta}\frac{\partial w}{\partial\eta};$$
$$\kappa_2=-\frac{1}{A_2}\frac{\partial}{\partial\eta}\left(\frac{1}{A_2}\frac{\partial w}{\partial\eta}\right)-\frac{1}{(A_1)^2A_2}\frac{\partial A_2}{\partial\xi}\frac{\partial w}{\partial\xi}; \quad (11)$$
$$\kappa_{12}=-\frac{1}{2}\left(\frac{A_2}{A_1}\frac{\partial}{\partial\xi}\left(\frac{1}{A_2^2}\frac{\partial w}{\partial\eta}\right)+\frac{A_1}{A_2}\frac{\partial}{\partial\eta}\left(\frac{1}{A_1^2}\frac{\partial w}{\partial\xi}\right)\right).$$

Step 6. If in equations (3 and 4) the terms depending on transverse shear forces are neglected, these equations are satisfied identically. By introducing the stress function Φ, the corresponding force components are given by

$$N_1=\frac{1}{A_2}\frac{\partial}{\partial\eta}\left(\frac{1}{A_2}\frac{\partial\Phi}{\partial\eta}\right)+\frac{1}{(A_1)^2A_2}\frac{\partial A_2}{\partial\xi}\frac{\partial\Phi}{\partial\xi};$$
$$N_2=\frac{1}{A_1}\frac{\partial}{\partial\xi}\left(\frac{1}{A_2}\frac{\partial\Phi}{\partial\xi}\right)+\frac{1}{(A_2)^2A_1}\frac{\partial A_1}{\partial\eta}\frac{\partial\Phi}{\partial\eta}; \quad (12)$$
$$T_h=-\frac{1}{A_1A_2}\left(\frac{\partial^2\Phi}{\partial\xi\partial\eta}-\frac{1}{A_1}\frac{\partial A_1}{\partial\eta}\frac{\partial\Phi}{\partial\xi}-\frac{1}{A_2}\frac{\partial A_2}{\partial\xi}\frac{\partial\Phi}{\partial\eta}\right).$$

Step 7. To derive the governing differential equations of elastic stability, it is necessary to introduce Hooke's law. It expresses the relationship between the normal strains ε_1, ε_2 and the shear strain ε_{12}, and the corresponding forces N_1, N_2, T_h through the stiffness parameters $\delta_i, i=\overline{1,4}, \delta_G$. In the case of symmetric rib stiffening, it takes the form

$$\begin{pmatrix}\varepsilon_1\\ \varepsilon_2\\ \varepsilon_{12}\end{pmatrix}=\begin{pmatrix}\delta_1 & \delta_3 & 0\\ \delta_3 & \delta_2 & 0\\ 0 & 0 & \delta_G\end{pmatrix}\begin{pmatrix}N_1\\ N_2\\ T_h\end{pmatrix}. \quad (13)$$

Step 8. Accordingly, the bending moments are expressed in terms of the changes in curvature and twisting of the midsurface

$$\begin{pmatrix}M\\ M_2\\ H_h\end{pmatrix}=\begin{pmatrix}D_1 & D_3 & 0\\ D_3 & D_2 & 0\\ 0 & 0 & D_G\end{pmatrix}\begin{pmatrix}\kappa_1\\ \kappa_2\\ \kappa_{12}\end{pmatrix}. \quad (14)$$

Step 9. The corresponding stiffness parameters in (13) and (14) are given by

$$\delta_1=\frac{\omega_2\left(1-\nu^2\right)}{Eh\left(\omega_1\omega_2-\nu^2\right)};\quad \delta_2=\frac{\omega_2\left(1-\nu^2\right)}{Eh\left(\omega_1\omega_2-\nu^2\right)};$$
$$\delta_3=\frac{\nu\left(1-\nu^2\right)}{Eh\left(\omega_1\omega_2-\nu^2\right)};\quad \delta_G=\frac{1}{Gh}; \quad (15)$$

$$D_1=\frac{Eh^3i_1}{12\left(1-\nu^2\right)};\quad D_2=\frac{Eh^3i_2}{12\left(1-\nu^2\right)};\quad D_3=\frac{Eh^3\nu}{12\left(1-\nu^2\right)};$$
$$D_G=\frac{Gh^3}{6};\quad G=\frac{E}{2\left(1+\nu\right)}. \quad (16)$$

The following steps are performed to reduce the above equations and expressions to a system of governing partial differential equations describing equilibrium under the given loading of the considered compound shell system, using automation in the Maple computer algebra system.

Step 10. The following steps are performed to reduce the above equations and expressions to a system of governing partial differential equations describing equilibrium under the given loading of the considered compound shell system. The procedure is implemented using automation in the Maple computer algebra system. From equations (6 and 7), the transverse forces Q_1 and Q_2 are determined. Substituting expressions (10 and 14) into (5) yields the first stability equation. Substitution of (13) into (9) yields the second equation, and both equations are formulated in terms of the normal displacement function w and the stress function Φ.

Stability equations of an eccentrically reinforced cylindrical segment. To obtain the stability equations of the considered system, equations (3–9) are implemented in the CAS.

For a cylindrical shell of medium length, satisfying the inequality $\sqrt{\frac{h}{R}}<\frac{L}{R}<\sqrt{\frac{R}{h}}$, dimensionless coordinates are introduced: $\overline{x}=\overline{s}/L$, $\overline{\varphi}=y/R$, where $\xi=\overline{s}$, $\eta = y$. When implementing these expressions in the CAS, the overbars in the notation are omitted. For the cylindrical shell, $A_1 = A_2 = 1$, $R_2 = R$. The combined loading and the curvatures of the midsurface are introduced according to (10), (11), while the stress functions are given by (12). The transverse forces Q_1 and Q_2 are expressed from equations (6, 7), denoted in the CAS as "uM1", "uM2", with temporary notation "QQ1(x, φ)", "QQ2(x, φ)".

$$Qq1 := solve(uM1, QQ1(x, \varphi)) :$$
$$Q1 := (x, \varphi) \to expand(simplify(Qq1)) :$$
$$Qq2 := solve(uM2, QQ2(x, \varphi)) :$$
$$Q2 := (x, \varphi) \to expand(simplify(Qq2)) :$$

The equilibrium equation (6), denoted as "uz", is written taking into account $R_1 = \infty$ in the form

$$Uz := expand(simplify(limit(uz, R1 = infinity)));$$

The bending moments in the form (14) are represented in the CAS as

$$m := Multiply\left(\begin{bmatrix} D1 & D3 & 0 \\ D3 & D2 & 0 \\ 0 & 0 & DG \end{bmatrix}, \begin{bmatrix} \kappa 1(x,\varphi) \\ \kappa 2(x,\varphi) \\ \kappa 12(x,\varphi) \end{bmatrix}\right):$$

where

$$M1 := (x,\varphi) \to m[1]: M2 := (x,\varphi) \to m[2]: Hh := (x,\varphi) \to m[3]:$$

and thus, the first equation of the governing stability equations system takes the form

$$U1 := collect(expand(simplify(Uz))), \{D1, D2, D3, DG\});$$

$$U1 := \frac{N20\left(\frac{\partial^2}{\partial\varphi^2} w(x,\varphi)\right)}{R^2} + \frac{N10\left(\frac{\partial^2}{\partial x^2} w(x,\varphi)\right)}{L^2} - \frac{D1\left(\frac{\partial^4}{\partial x^4} w(x,\varphi)\right)}{L^4} - \frac{D2\left(\frac{\partial^4}{\partial\varphi^4} w(x,\varphi)\right)}{R^4} - \frac{2\,D3\left(\frac{\partial^4}{\partial x^2\partial\varphi^2} w(x,\varphi)\right)}{L^2R^2} - \frac{2\,DG\left(\frac{\partial^4}{\partial x^2\partial\varphi^2} w(x,\varphi)\right)}{L^2R^2} + \frac{\frac{\partial^2}{\partial x^2}\Phi(x,\varphi)}{L^2R}$$

Hooke's law equations (13) yield the second equation of the governing system, also taking into account $R_1 = \infty$

$$MM := Multiply\left(\begin{bmatrix} \delta 1 & \delta 3 & 0 \\ \delta 3 & \delta 2 & 0 \\ 0 & 0 & \delta G \end{bmatrix}, \begin{bmatrix} N1(x,\varphi) \\ N2(x,\varphi) \\ Th(x,\varphi) \end{bmatrix}\right):$$

$$\varepsilon 1 := (x,\varphi) \to MM[1]: \varepsilon 2 := (x,\varphi) \to MM[2]: \varepsilon 12 := (x,\varphi) \to MM[3]: sl := \{\delta 1, \delta 2, \delta 3, \delta G\}:$$

$$U2 := collect(expand(simplify(limit(usd, R1 = infinity)))), sl);$$

$$U2 := \frac{\frac{\partial^2}{\partial x^2} w(x,\varphi)}{L^2R} + \frac{\left(\frac{\partial^4}{\partial\varphi^4}\Phi(x,\varphi)\right)\delta 1}{R^4} + \frac{2\left(\frac{\partial^4}{\partial x^2\partial\varphi^2}\Phi(x,\varphi)\right)\delta 3}{L^2R^2} + \frac{\left(\frac{\partial^4}{\partial x^2\partial\varphi^2}\Phi(x,\varphi)\right)\delta G}{L^2R^2} + \frac{\left(\frac{\partial^4}{\partial x^4}\Phi(x,\varphi)\right)\delta 2}{L^4}$$

As a result, the complete system of partial differential equations describing the equilibrium of the reinforced cylindrical shell is obtained

$$\begin{cases} \dfrac{D_1}{L^4}\dfrac{\partial^4 w_{cyl}}{\partial\bar{x}^4} + 2\dfrac{D_3 + D_G}{l^2R^2}\dfrac{\partial^4 w_{cyl}}{\partial\bar{x}^2\partial\bar{\varphi}^2} + \dfrac{D_2}{R^4}\dfrac{\partial^4 w_{cyl}}{\partial\bar{\varphi}^4} = \\ = \dfrac{1}{L^2R}\dfrac{\partial^2\Phi_{cyl}}{\partial\bar{x}^2} + \dfrac{N_{10}}{L^2}\dfrac{\partial^2 w_{cyl}}{\partial\bar{x}^2} + \dfrac{N_{20}}{R^2}\dfrac{\partial^2 w_{cyl}}{\partial\bar{\varphi}^2} \\ \dfrac{\delta_1}{R^4}\dfrac{\partial^4\Phi_{cyl}}{\partial\bar{\varphi}^4} + 2\dfrac{\delta_3 + \delta_G}{L^2R^2}\dfrac{\partial^4\Phi_{cyl}}{\partial\bar{x}^2\partial\bar{\varphi}^2} + \dfrac{1}{L^2R}\dfrac{\partial^2 w_{cyl}}{\partial\bar{x}^2} = 0 \end{cases}. \quad (17)$$

The parameters of the reinforcing load-carrying elements of the shell in the CAS are defined by formulas (15, 16)

$$\delta 1 := \frac{\omega 2\cdot(1-\upsilon^2)}{E\cdot h\cdot(\omega 1\cdot\omega 2-\upsilon^2)}: \delta 2 := \frac{\omega 1\cdot(1-\upsilon^2)}{E\cdot h\cdot(\omega 1\cdot\omega 2-\upsilon^2)}:$$

$$\delta 3 := \frac{-\upsilon\cdot(1-\upsilon^2)}{E\cdot h\cdot(\omega 1\cdot\omega 2-\upsilon^2)}: \delta G := \frac{(1)}{G\cdot h}:$$

$$D1 := \frac{E\cdot h^3\cdot i1}{12\cdot(1-\upsilon^2)}: D2 := \frac{E\cdot h^3\cdot i2}{12\cdot(1-\upsilon^2)}:$$

$$D3 := \frac{\upsilon\cdot E\cdot h^3}{12\cdot(1-\upsilon^2)}: DG := \frac{G\cdot h^3}{6}: G := \frac{E}{2\cdot(1+\upsilon)}:$$

The next step involves introducing the geometric parameters of the shell $\varepsilon_c = h/R$, $K = L/R$, and the external load according to (10), expressed in terms of the external pressure q uniformly distributed over the surface of the structure and the axial force T, with the membrane forces in the midsurface $N_{10} = T/R$, $N_{20} = qR$, and dimensionless forces.

$$\eta_{cyl} = \frac{T}{Eh^2}; \quad \chi_{cyl} = \frac{qR^2}{Eh^2}, \quad (18)$$

which in the CAS is written as

$$N10 := -\frac{T}{R}: T := \eta\cdot E\cdot h^2: N20 := -q\cdot R:$$

$$q := \frac{\chi\cdot E\cdot h^2}{R^2}: h := \varepsilon c\cdot R: L := K\cdot R:$$

The normal displacement function w_{cyl} and the stress function Φ_{cyl} are defined by [1]

$$w_{cyl}(\bar{x},\bar{\varphi}) = W_{cyl}(\bar{x})\cdot\cos(n\bar{\varphi}); \quad (19)$$

$$\Phi_{cyl}(\bar{x},\bar{\varphi}) = Eh^2\,\bar{\Phi}_{cyl}(\bar{x})\cdot\cos(n\bar{\varphi}),$$

which are represented in the CAS as

$$w := (x,\varphi) \to ww(x)\cdot\cos(n\cdot\varphi):$$

$$\Phi := (x,\varphi) \to \Phi\varphi(x)\cdot\cos(n\cdot\varphi):$$

Further elementary transformations are performed on system (17), denoted in the CAS as "U1" and "U2"

$$SS1 := ww(x), \left(\frac{d^2}{dx^2} ww(x)\right), \left(\frac{d^4}{dx^4} ww(x)\right), \Phi\varphi(x):$$

$$SS2 := \left(\frac{d^2}{dx^2}\Phi\varphi(x)\right), \left(\frac{d^4}{dx^4}\Phi\varphi(x)\right), R, E, K, n, \varepsilon c, \chi, \eta:$$

$$SSS := [SS1, SS2]:$$

$$eq1 := collect\left(expand\left(simplify\left(\frac{U1\left(-1+\upsilon^2\right)R}{\varepsilon c^2\cdot\cos(n\varphi)\cdot E}\right)\right), SSS\right);$$

$$eq1 := \left(\frac{1}{12}\varepsilon c\,i2\,n^4 + \left(\upsilon^2-1\right)\chi n^2\right)ww(x) + \frac{\left(-\frac{1}{6}\varepsilon c\,n^2 + \left(-\upsilon^2+1\right)\eta\right)\left(\frac{d^2}{dx^2} ww(x)\right)}{K^2} + \frac{1}{12}\frac{\varepsilon c\,i1\left(\frac{d^4}{dx^4} ww(x)\right)}{K^4} + \frac{\left(\upsilon^2-1\right)\left(\frac{d^2}{dx^2}\Phi\varphi(x)\right)}{\varepsilon c^2 K^2 E R^2}$$

$$Up := \frac{R^5 E\cdot U2\cdot\left(\omega 1\,\omega 2-\upsilon^2\right)\cdot\varepsilon c}{\cos(n\varphi)\cdot\omega 2\cdot n^4}:$$

$$eq2 := collect(expand(simplify(Up)), SSS);$$

$$eq2 := \frac{\left(\omega 1-\frac{\upsilon^2}{\omega 2}\right)\varepsilon c\,E\,R^2\left(\frac{d^2}{dx^2} ww(x)\right)}{n^4K^2} + \left(-\upsilon^2+1\right)\Phi\varphi(x) + \frac{\left(\frac{2\upsilon^2}{\omega 2}+\frac{2\upsilon}{\omega 2}-2\,\omega 1\,\upsilon-2\,\omega 1\right)\left(\frac{d^2}{dx^2}\Phi\varphi(x)\right)}{n^2K^2} + \frac{\left(-\frac{\omega 1\,\upsilon^2}{\omega 2}+\frac{\omega 1}{\omega 2}\right)\left(\frac{d^4}{dx^4}\Phi\varphi(x)\right)}{n^4K^4}$$

After the transformations, a system of differential equations in terms of functions W_{cyl}, $\bar{\Phi}_{cyl}$ is obtained

$$\begin{cases} \left(\frac{\varepsilon_c i_2 n^2}{\Omega} - \chi_{cyl}\right) n^2 W_{cyl}(\bar{x}) + \left(-\frac{2\varepsilon_c n^2}{\Omega} + \eta_{cyl}\right)\frac{W''_{cyl}(\bar{x})}{K^2} - \\ -\frac{\varepsilon_c i_1}{\Omega K^4} W^{IV}_{cyl}(\bar{x}) = \frac{1}{(RK\varepsilon_c)^2 E}\bar{\Phi}''_{cyl}(\bar{x}) \\ \frac{ER^2\varepsilon_c(\omega_1\omega_2 - \nu^2)}{\omega_2 n^4 K^2(1-\nu^2)} W''_{cyl}(\bar{x}) + \frac{\omega_1}{\omega_2 n^4 K^4}\bar{\Phi}^{IV}_{cyl}(\bar{x}) + \\ +\frac{2(\omega_1\omega_2 - \nu)}{\omega_2 n^2 K^2(\nu - 1)}\bar{\Phi}''_{cyl}(\bar{x}) + \bar{\Phi}_{cyl}(\bar{x}) = 0 \end{cases}. \quad (20)$$

In equation (20), $\Omega = 12(1-\nu^2)$.

Since for the considered class of shells the parameters satisfy $K^2 > 1$, $n^2 \gg 1$, in the second equation of system (20) terms of order $1/(K^2 n^2)$ and higher can be neglected. Accordingly, the function $\bar{\Phi}_{cyl}(\bar{x})$ can be expressed, yielding the resulting governing equation

$$sl1 := \left(\frac{E\,\varepsilon c\,R^2\,(\omega 1\,\omega 2 - \nu^2)}{n^4\,K^2\,\omega 2\,(1-\nu^2)}\right)\left(\frac{d^2}{dx^2}\,ww(x)\right):$$

$$eq22 := sl1 + \Phi\varphi(x):$$

$$r := solve(eq22, \Phi\varphi(x)); \Phi\varphi := x \to r:$$

$$SSS1 := \left\{ww(x), \left(\frac{d^2}{dx^2}\,ww(x)\right), \left(\frac{d^4}{dx^4}\,ww(x)\right)\right\}:$$

$$Req := collect\left(expand\left(\frac{n^4\,eq1\,K^4\,\varepsilon c}{1-\nu^2}\right), SSS1\right);$$

$$Req := \left(\frac{1}{12}\frac{n^4\,\varepsilon c^2\,i1}{-\nu^2+1} + \frac{\omega 1}{-\nu^2+1} - \frac{\nu^2}{(-\nu^2+1)\,\omega 2}\right)\left(\frac{d^4}{dx^4}\,ww(x)\right)$$
$$+\left(-\frac{1}{6}\frac{n^6 K^2\,\varepsilon c^2}{-\nu^2+1} - \frac{n^4 K^2\,\varepsilon c\,\eta\,\nu^2}{-\nu^2+1} + \frac{n^4 K^2\,\varepsilon c\,\eta}{-\nu^2+1}\right)\left(\frac{d^2}{dx^2}\,ww(x)\right)$$
$$+\left(\frac{1}{12}\frac{n^8 K^4\,\varepsilon c^2\,i2}{-\nu^2+1} + \frac{n^6 K^4\,\varepsilon c\,\chi\,\nu^2}{-\nu^2+1} - \frac{n^6 K^4\,\varepsilon c\,\chi}{-\nu^2+1}\right)ww(x)$$

After simplification, the governing differential equation of the primary stress state with respect to the deflection function of the cylindrical shell reinforced with two-sided ribs takes the form

$$\left(\frac{\varepsilon_c i_2 n^2}{\Omega} - \chi_{cyl}\right) n^6 \varepsilon_c K^4 W_{cyl}(\bar{x}) + \left(-\frac{2\varepsilon_c n^2}{\Omega} + \eta_{cyl}\right) \times$$
$$\times n^4 \varepsilon_c K^2 W''_{cyl}(\bar{x}) + \left(\frac{\omega_1\omega_2 - \nu^2}{\omega_2(1-\nu^2)} + \frac{\varepsilon_c^2 i_1 n^4}{\Omega}\right) W^{IV}_{cyl}(\bar{x}) = 0. \quad (21)$$

For parameter values $i_1 = i_2 = \omega_1 = \omega_2 = 1$, the equation reduces to that of an unreinforced cylindrical shell, as presented in [1, 8].

Governing system of partial differential equations for a symmetrically reinforced conical shell. A dimensionless coordinate $x = s/l_1$ is introduced with base coordinates $\xi = s$, $\eta = \varphi$. To use the equations derived for the cylindrical shell, for the conical shell in equations and expressions (3–14), the following substitutions are introduced in the CAS

$$L := l1 : R := l1 :$$

For the conical shell, the following expressions hold: $A_1 = 1$, $A_2 = x\cos\alpha$, $R_2 = l_1 x\,\mathrm{tg}\,\alpha$, while $R_1 = \infty$.

To represent the transverse forces Q_1 and Q_2, the same operators in Maple are used as for the cylindrical shell. In the equilibrium equation "uz", taking into account $R_1 = \infty$, we obtain

$$Uz := expand(simplify(limit(uz, R1 = infinity)));$$

The CAS representation of Hooke's law and expressions for bending moments remains unchanged. In the second equation, the condition : is also taken into account

$$SSS := \{D1, D2, D3, DG, N20, l1\};$$
$$U1 := collect\left(expand\left(simplify\left(Uz\cdot\frac{l1^4}{x\cos(\alpha)}\right)\right), SSS\right);$$
$$SS1 := simplify(limit(usd\cdot l1^4, R1 = infinity)):$$
$$SS2 := \{\delta 1, \delta 2, \delta 3, \delta G\}:$$
$$U2 := collect(expand(SS1), SS2);$$

Thus, the complete system of partial differential equations describing the equilibrium of the reinforced conical segment is obtained

$$\begin{cases} -D_1\left(\frac{\partial^4 w_{cone}}{\partial x^4} + \frac{2}{x}\frac{\partial^3 w_{cone}}{\partial x^3}\right) - 2\frac{D_3 + D_G}{x^2\cos^2\alpha}\left(\frac{\partial^4 w_{cone}}{\partial x^2\partial\varphi^2} - \right. \\ \left. -\frac{1}{x}\frac{\partial^2 w_{cone}}{\partial x\partial\varphi^2} + \frac{1}{x^2}\frac{\partial^2 w_{cone}}{\partial\varphi^2}\right) - \frac{D_2}{x^2}\left(\frac{1}{x^2\cos^4\alpha}\frac{\partial^4 w_{cone}}{\partial\varphi^4} + \right. \\ \left. +\frac{2}{x^2\cos^2\alpha}\frac{\partial^2 w_{cone}}{\partial\varphi^2} - \frac{\partial^2 w_{cone}}{\partial x^2} + \frac{1}{x}\frac{\partial w_{cone}}{\partial x}\right) + \\ +\frac{l_1\,\mathrm{tg}\,\alpha}{x}\frac{\partial^2\Phi_{cone}}{\partial x^2} + N_{10} l_1^2\frac{\partial^2 w_{cone}}{\partial x^2} + \\ +\frac{N_{20} l_1^2}{x}\left(\frac{1}{x\cos^4\alpha}\frac{\partial^2 w_{cone}}{\partial\varphi^2} + \frac{\partial w_{cone}}{\partial x}\right) = 0 \\ \frac{\delta_1}{x^2}\left(\frac{1}{x^2\cos^4\alpha}\frac{\partial^4\Phi_{cone}}{\partial\varphi^4} + \frac{2}{x^2\cos^2\alpha}\frac{\partial^2\Phi_{cone}}{\partial\varphi^2} - \right. \\ \left. -\frac{\partial^2\Phi_{cone}}{\partial x^2} + \frac{1}{x}\frac{\partial\Phi_{cone}}{\partial x}\right) + 2\frac{\delta_3 + \delta_G}{x^2\cos^2\alpha}\left(\frac{\partial^4\Phi_{cone}}{\partial x^2\partial\varphi^2} + \right. \\ \left. +\frac{1}{x}\frac{\partial^3\Phi_{cone}}{\partial x\partial\varphi^2} + \frac{1}{x^2}\frac{\partial^2\Phi_{cone}}{\partial\varphi^2}\right) + \delta_2\left(\frac{\partial^4\Phi_{cone}}{\partial x^4} + \right. \\ \left. +\frac{2}{x}\frac{\partial^3\Phi_{cone}}{\partial x^3}\right) + \frac{l_1\,\mathrm{tg}\,\alpha}{x}\frac{\partial^2 w_{cone}}{\partial x^2} = 0 \end{cases}. \quad (22)$$

It should be noted that the reinforcement parameters given by (15, 16) coincide in the CAS for both shell types. The force expressions in (10) for the conical shell are written as

$$N_{10} = \frac{q}{2\,\mathrm{tg}\,\alpha}\left(\frac{l_0^2}{l_1 x} - x l_1\right) - \frac{T}{\pi l_1 x \sin 2\alpha}; \quad N_{20} = -\frac{q l_1 x}{tg\,\alpha}.$$

The radial displacement and stress functions are defined as

$$w_{cone}(x, \varphi) = W_{cone}(x)\,\mathrm{tg}\,\alpha\,\cos n\varphi; \quad (23)$$
$$\Phi_{cone}(x, \varphi) = \bar{\Phi}_{cone}(x)\varepsilon^2 l_1 Eh\,\mathrm{tg}^2\,\alpha\cos n\varphi.$$

Further calculations use the dimensionless parameters

$$\delta = \frac{n^2}{\cos^2\alpha}; \quad p = \varepsilon\delta; \quad \varepsilon = \sqrt{\frac{h\,\mathrm{ctg}\,\alpha}{l_1\sqrt{12(1-\nu^2)}}};$$
$$\chi_{cone} = \frac{q l_1}{Eh\varepsilon^3\,\mathrm{tg}^3\,\alpha}; \quad \eta_{cone} = \frac{T\cos\alpha}{2\pi Eh\varepsilon^2 l_1\sin^3\alpha}. \quad (24)$$

Elementary transformations of system (22) are performed using the CAS, yielding the required system in

terms of W_{cone}, $\bar{\Phi}_{cone}$

$$\begin{cases}\left(\frac{2\varepsilon i_2+2\varepsilon-pi_2}{x^3}+\chi_{cone}\right)W_{cone}(x)+\left(-\frac{2p+\varepsilon i_2}{px^2}-\right.\\ \left.-\frac{x\chi_{cone}}{p}\right)\varepsilon W'_{cone}(x)+\left(\frac{(l_0/l_1)^2-x^2}{2p}\varepsilon\chi_{cone}+\frac{2\varepsilon}{x}+\right.\\ \left.+\frac{\varepsilon^2 i_2}{xp}-\frac{\eta_{cone}}{p}\right)W''_{cone}(x)+\frac{1}{p}\left(\Phi''_{cone}(x)-\right.\\ \left.-2\varepsilon^2 i_1 W''_{cone}(x)-x\varepsilon^2 i_1 W^{IV}_{cone}(x)\right)=0\\ \frac{\omega_1\omega_2-\nu^2}{xp\left(\nu^2-1\right)}W''_{cone}(x)-\frac{\varepsilon\omega_1}{p}\bar{\Phi}^{IV}_{cone}(x)-\frac{2\varepsilon\omega_1}{xp}\bar{\Phi}''_{cone}(x)+\\ +\frac{2(\omega_1\omega_2-\nu)p+\varepsilon\omega_2(1-\nu)}{x^2p(\nu-1)}\varepsilon\left(\frac{1}{x}\bar{\Phi}'_{cone}(x)-\right.\\ \left.-\bar{\Phi}''_{cone}(x)\right)-\frac{2\varepsilon(\omega_1\omega_2-\nu+\omega_2-\nu\omega_2)+p\omega_2(\nu-1)}{x^4(\nu-1)}\times\\ \times\bar{\Phi}_{cone}(x)=0\end{cases}. \quad (25)$$

For a thin reinforced conical shell, the presence of a small parameter $\varepsilon \ll 1$ allows simplification of system (25) using CAS operators

$$UU1 := simplify(U1, \{\varepsilon = 0\}) :$$
$$UU2 := simplify(U2, \{\varepsilon = 0\}) :$$

This leads to a simplified system

$$\begin{cases}\left(\chi_{cone}-\frac{pi_2}{x^3}\right)W_{cone}(x)-\frac{\eta_{cone}}{p}W''_{cone}(x)+\frac{1}{p}\bar{\Phi}''_{cone}(x)=0\\ \frac{\omega_1\omega_2-\nu^2}{xp(\nu^2-1)}W''_{cone}(x)-\frac{p\omega_2}{x^4}\bar{\Phi}_{cone}(x)=0\end{cases}.$$

From the second equation of this system, the function $\bar{\Phi}_{cone}$, is expressed, leading to the desired governing equation. The corresponding actions are performed in the CAS

$$r := solve(UU2, \Phi\Phi(x)); \Phi\Phi := x \to r;$$
$$R1 := factor(expand(UU1)) :$$
$$p1 := ww(x), \left(\frac{d}{dx}ww(x)\right), \left(\frac{d^2}{dx^2}ww(x)\right) :$$
$$p2 := \left(\frac{d^3}{dx^3}ww(x)\right), \left(\frac{d^4}{dx^4}ww(x)\right) :$$
$$p4 := [p1, p2, p3] : Req := collect(R1, p4);$$
$$Req := \left(-\frac{(\omega 2\,\upsilon^2-\omega 2)\,p^3\chi}{(-1+\upsilon)(1+\upsilon)\,\omega 2\,x^3}-\frac{(-\omega 2\,\upsilon^2+\omega 2)\,i2\,p^4}{x^6(-1+\upsilon)(1+\upsilon)\,\omega 2}\right)ww(x)+\left(\right.$$
$$\left.-\frac{(-\omega 2\,\upsilon^2+\omega 2)\,p^2\eta}{(-1+\upsilon)(1+\upsilon)\,\omega 2\,x^3}-\frac{6\,\omega 1\,\omega 2-6\,\upsilon^2}{(-1+\upsilon)(1+\upsilon)\,\omega 2\,x^2}\right)\left(\frac{d^2}{dx^2}ww(x)\right)$$
$$-\frac{(6\,\omega 1\,\omega 2-6\,\upsilon^2)\left(\frac{d^3}{dx^3}ww(x)\right)}{(-1+\upsilon)(1+\upsilon)\,\omega 2\,x}-\frac{(\omega 1\,\omega 2-\upsilon^2)\left(\frac{d^4}{dx^4}ww(x)\right)}{(-1+\upsilon)(1+\upsilon)\,\omega 2}$$

After simplification, the governing equation for the deflection function W_{cone} of the symmetrically reinforced conical segment takes the form

$$\frac{\omega_1\omega_2-\nu^2}{\omega_2(1-\nu^2)}W^{IV}_{cone}(x)+\frac{6(\omega_1\omega_2-\nu^2)}{x^2\omega_2(1-\nu^2)}W'''_{cone}(x)+$$
$$+\left(\frac{6(\omega_1\omega_2-\nu^2)}{x^2\omega_2(1-\nu^2)}+\frac{p^2\eta_{cone}}{x^3}\right)W''_{cone}(x)+ \quad (26)$$
$$+\left(\frac{pi_2}{x^6}-\frac{p^3\chi_{cone}}{x^3}\right)W_{cone}(x)=0.$$

For $i_1 = i_2 = \omega_1 = \omega_2 = 1$, the equations reduce to those of an unreinforced conical shell [1, 8]. It should be noted that in practical calculations, equations (21) and (26) are expressed in terms of external loads T, q using substitutions for bending moments (18 and 24).

Governing equations for segments reinforced with one-sided stiffening. The difference in derivation for one-sided reinforcement is introduced in equations (2). Additional terms are taken into account via (13, 14). Using the CAS, analogous steps are performed as in the previous procedure. The key difference is that, in deriving the governing equation for the conical shell, terms containing ε^2 are neglected while retaining those with the small parameter ε.

The associated equations corresponding to (21) and (26) are given by (27) and (28). Thus, the governing equation for the cylindrical shell with one-sided reinforcement is

$$b_0 W_{cyl}(\bar{x})+b_2 W''_{cyl}(\bar{x})+b_4 W^{IV}_{cyl}(\bar{x})=0, \quad (27)$$

where

$$b_0=\left(\frac{\varepsilon_c i_2 n^2}{\Omega}-\chi_{cyl}\right)n^6\varepsilon_c K^4-\lambda_2^2\frac{n^6\varepsilon_c^2}{\omega_2}(1-\nu^2);$$
$$b_2=\left(-\frac{2\varepsilon_c n^2}{\Omega}+\eta_{cyl}\right)n^4\varepsilon_c K^2+$$
$$+\left(\lambda_2\frac{n^2\varepsilon_c(1-\nu^2)}{\omega_1\omega_2-\nu^2}-1\right)\lambda_2 n^4\varepsilon_c\nu K^2;$$
$$b_4=\frac{\omega_1\omega_2-\nu^2}{\omega_2(1-\nu^2)}+\frac{\varepsilon_c^2 i_1 n^4}{\Omega}-$$
$$-\frac{\lambda_1\lambda_2 n^4\nu^2\varepsilon_c^2}{\omega_2(\omega_1\omega_2-\nu^2)}(\nu^4-2\omega_1\omega_2(1-\nu^2)),$$

and for the conical shell

$$a_0(x)W_{cone}(x)+a_1(x)W'_{cone}(x)+a_2(x)W''_{cone}(x)+$$
$$+a_3(x)W'''_{cone}(x)+a_4(x)W^{IV}_{conel}(x)=0, \quad (28)$$

where

$$a_0(x)=p^3\left(\frac{i_2(p-2\varepsilon)}{x^6}-\left(\frac{\chi_{cone}}{x^3}+\frac{2\varepsilon}{x^6}\right)+\right.$$
$$\left.+\lambda_2^2\frac{12(2\varepsilon-p)}{x^6}(1-\nu^2)^2\right);$$
$$a_1(x)=\varepsilon p^2\left(\frac{2p}{x^5}+\frac{\chi_{cone}}{x^2}\right);$$
$$a_2(x)=\frac{6(\omega_1\omega_2-\nu^2)}{x^2\omega_2(1-\nu^2)}+\frac{p^2\eta_{cone}}{x^3}-\frac{2p^3\varepsilon}{x^4}+$$
$$+\frac{p^2\varepsilon\chi_{cone}}{2x}\left(1-\frac{(l_0/l_1)^2}{x^2}\right)-2\lambda_1\frac{p\varepsilon\sqrt{\Omega}}{x^3}-$$
$$-2\lambda_2\frac{p\sqrt{\Omega}}{x^3\omega_2}(p\nu+\varepsilon(2\omega_1-\nu))+$$
$$+12\lambda_2\frac{\nu\varepsilon p^3(\lambda_2\omega_1-\lambda_1\omega_2)}{x^4\omega_2(\omega_1\omega_2-\nu^2)}(1-\nu^2)^2;$$
$$a_3(x)=\frac{6(\omega_1\omega_2-\nu^2)}{x\omega_2(1-\nu^2)}-\frac{2p\varepsilon\sqrt{\Omega}}{x^2\omega_2}(3\lambda_2\omega_1+2\lambda_1\omega_2);$$

$$a_4(x)=\frac{\omega_1\omega_2-\nu^2}{\omega_2(1-\nu^2)}-\frac{p\varepsilon\sqrt{\Omega}}{x\omega_2}(\lambda_2\omega_1+\lambda_1\omega_2).$$

If in (27 and 28) one sets $\lambda_1=\lambda_2=0$, and in (28) neglects terms containing ε, then equations (21 and 26) are recovered for cylindrical and conical shells, respectively. The coefficients C_1, C_2, defining the eccentricity of the reinforcing system, generalize cases for numerical analysis.

Differential continuity conditions across ring stiffeners and boundary conditions. In the continuity conditions across a ring stiffener, the stiffness parameters are defined as

$$G^*_{cone,1}=\frac{G_1}{\cos^3\alpha};\quad G^*_{cone,2}=\frac{G_2}{\cos\alpha};\quad G^*_{cyl,1}=G_1;\quad G^*_{cyl,2}=G_2;$$

$$G_1=\frac{n^4(n^2-1)^2}{EhR^3_{ring}}(EJ)^{ring}_x;\quad G_1=\frac{n^2(n^2-1)^2}{EhR^3_{ring}(n^2+1)}(EJ)^{ring}_z,$$

where J^{ring}_x, J^{ring}_z are the moments of inertia of the ring stiffener in the plane of initial curvature and out of this plane, respectively.

Following [1, 13], connecting ring stiffeners are placed at the edges of both conical and cylindrical segments, each providing half of the stiffness, and the compatibility conditions take the form

$$W_{cone}(1)=W_{cyl}(0);\quad W'_{cone}(1)=W'_{cyl}(0);$$

$$W''_{cone}(1)+\frac{1}{2}G^*_{cone,2}W'_{cone}(1)=W''_{cyl}(0)+\frac{1}{2}G^*_{cyl,2}W'_{cyl}(0);$$

$$W'''_{cone}(1)-\frac{1}{2}G^*_{cone,1}W_{cone}(1)=W'''_{cyl}(0)+\frac{1}{2}G^*_{cyl,1}W_{cyl}(0). \quad (29)$$

The boundary conditions for the considered compound shell system correspond to simply supported edges.

Solution methods. *Application of the finite difference method and computer visualization of local and global bifurcation modes*. To solve the problem using equations (21), (27), (26), (28) and relations (29) with boundary conditions, the finite difference method reduces the problem to difference equations for section deflections at grid nodes.

The interval $[a; b]$ is divided into N equal parts, with step $= (b-a)/N$. For the cylindrical segment, $[a; b] = [0; 1]$, and for the conical segment $[a; b] = [x_0; 1]$, where $x_0 = l_0/(l_1)$. At interior points, derivatives of the deflection function are approximated by fourth-order central differences. At the boundaries, second-order finite differences are used. In the coupling equations, third-order one-sided finite differences are applied: forward differences for the left-hand sides and backward differences for the right-hand sides of (29) [1].

The finite difference formulas and node numbering schemes are detailed in [1, 8]. The algorithm for computer visualization [13] of bifurcation modes of the reinforced compound shell system "cone-cylinder" consists of the following stages.

Stage 1. A homogeneous system of linear algebraic equations is formed. Its determinant $\Delta(T, q, n)$ is extracted. For a fixed axial force T, the wave number n is found such that the pressure q is the smallest positive root of the characteristic equation $\Delta(T, q, n) = 0$. This yields the critical pressure corresponding to T.

Stage 2. The parameters T, q, n are substituted into the system, where one equation is made nonhomogeneous. The solution is normalized and scaled to obtain suitable visualization, resulting in a set $\{y[i]\}$ of deflection values.

Stage 3. For visualization of the bifurcation mode of the conical section, representation (23) is used: $w_{cone}(x, \varphi) = W_{cone}(x)\ \mathrm{tg}\alpha\ \cos n\varphi$. In polar coordinates, the interval $[0; 2\pi]$ of the polar angle φ is divided into 100 parts, and a surface frame of the post-buckling conical shell is constructed in the CAS

$$x0 := \frac{l0}{l1} : xB := x0 + \frac{(ii-1)\cdot(1-x0)}{\mathrm{N}-1} :$$

$$B := l1\cdot\mathrm{xB}\cdot\sin(\alpha) : sss := \frac{2\cdot\mathrm{Pi}}{100}\cdot(jj-1) :$$

$$\mathrm{A} := \mathrm{R}\cdot\mathrm{xB} + yy[ii]\cdot\sin(\alpha)\cdot\cos(n\cdot sss) :$$

$$sss1 := seq([[(\cos(\mathrm{sss})\cdot\mathrm{A},\ \sin(\mathrm{sss})\cdot\mathrm{A},\ \boldsymbol{B})], ii = 1..\mathrm{N}) :$$

$$gg := [seq([sss1], jj = 1..101)] :$$

Visualization is performed using

$$par1 := axes = none, lightmodel = \text{"light2"} :$$

$$par2 := orientation = [60, -0, 100], \mathrm{shading} = \mathrm{XYZ} :$$

$$GG := surfdata(gg, \mathrm{par1}, \mathrm{par2}, \mathrm{style} = surface) :$$

Stage 4. For the cylindrical section, representation (19) is used: $w_{cyl}(\bar{x}, \bar{\varphi}) = W_{cyl}(\bar{x})\cdot\cos(n\bar{\varphi})$. Taking into account geometry and node arrangement, the surface frame and visualization are defined in the CAS

$$\mathrm{B} := \frac{L\cdot(\mathrm{ii}-1)}{\mathrm{N}-1} : A := R + yy[ii + \mathrm{N} + 2]\cdot\cos(\mathrm{n}\cdot\mathrm{sss}) :$$

$$sss1 := seq([A\cdot\cos(sss), A\cdot\sin(\mathrm{sss}), \mathrm{B} + l1\cdot\sin(\alpha)], ii = 1..\mathrm{N}) :$$

$$GG1 := surfdata(gg, \mathrm{par1}, \mathrm{par2}, \mathrm{style} = surface) :$$

Stage 5. Ring stiffeners are visualized using the above procedure by selecting index ranges from 1 to 2 for the cylindrical section and from $N-1$ to N for the conical section.

Stage 6. Combined visualization of all surfaces is achieved using the "display" operator.

Analysis of numerical results. A comparative numerical analysis showed that the deviation in results for $N = 30$ and $N = 50$ is about 2 %. Therefore, $N = 30$ was adopted for computations. The numerical analysis was performed for shells with parameters: $l_1 = 1.82$ m and $h = 3\cdot10^{-3}$ m, $\alpha = 75°$, $\nu = 0.32$, $E = 68.64655$ GPa.

For the considered structures (single- or two-compartment), the radius of the cylinder was taken equal to the radius of the lower base of the truncated cone $R = l_1\cos\alpha$, with the dimensionless axial force parameter $T^* = \frac{T}{Eh^2}$ and the auxiliary parameter of external pressure $q^* = q\cdot10^{-5}$ (Pa).

For one-sided reinforcement, the rib width was taken as $b_1 = b_2 = 2h$, and the height as $\delta^p_1 = \delta^p_2 = 4h$. For two-sided symmetric reinforcement, the rib dimensions $\tilde{b}_1, \tilde{b}_2, \tilde{\delta}^p_1, \tilde{\delta}^p_2$ were determined from the condition of equal stiffness relative to the one-sided case, which reduces to equality of the moments of inertia of the ribs with respect to the axes lying in the midsurface. For example, for ring stiffeners, the following equation is obtained

$$\frac{1}{12}b_1(\delta^p_1)^3+\frac{1}{4}b_1\delta^p_1(h+\delta^p_1)^2 = 2\left(\frac{1}{12}\tilde{b}_1\left(\tilde{\delta}^p_1\right)^3+\frac{1}{4}\tilde{b}_1\tilde{\delta}^p_1\left(h+\tilde{\delta}^p_1\right)^2\right). \quad (30)$$

Two types of two-sided reinforcement were considered:

- *type 1* – the rib width is the same for one-sided and two-sided reinforcement $b_1 = b_2 = \tilde{b}_1 = \tilde{b}_2 = 2h$; then, from (30), the rib height for two-sided reinforcement is determined as $\tilde{\delta}_1^p = \tilde{\delta}_2^p = k_1 h$, yielding $k_1 = 3.0732$;

- *type 2* – the rib heights are equal $\delta_1^p = \delta_2^p = \tilde{\delta}_1^p = \tilde{\delta}_2^p = 4h$; the rib width for two-sided reinforcement is determined as $\tilde{b}_1 = \tilde{b}_2 = k_2 h$, where (30) gives $k_2 = 1$.

Let $k_{cyl,st}$, $k_{cone,st}$ denote the number of stringers, and $k_{cyl,rings}$, $k_{cone,rings}$ – the number of ring stiffeners for the cylindrical and conical segments, respectively. For the cylindrical shell, ring stiffeners and stringers are uniformly distributed along the generatrix and along ring directions, respectively, so that $t_2 = L/k_{cyl,rings}$, $t_1 = 2\pi R/k_{cyl,st}$. For the conical shell, ring stiffeners are uniformly distributed, $t_2 = (l_1 - l_0)/k_{cone,rings}$, while stringers are arranged along the generatrices, and the spacing $t_1 = (2\pi l_1 x \cos\alpha)/k_{cone,st}$ is variable and depends on x, which is taken into account in forming the difference equations. For the compound "cone–cylinder" structure, the number of stringers in both segments is taken to be the same.

Tables 1 and 2 present the critical pressure values depending on the number of stiffening ribs for one- and two-sided reinforcement at $T^* = 0$.

It should be noted that the number of ring stiffeners significantly affects the load-bearing capacity of the segments in terms of stability, whereas the number of stringers has a minor influence on the critical pressure in the considered cases, as also noted in [7, 11]. In the studied cases, external reinforcement leads to higher stability compared to internal placement of stiffening ribs, which is consistent with [11, 25].

In many cases considered, two-sided reinforcement provides higher critical pressure values compared to the corresponding equally stiff one-sided reinforcement. However, for a cylindrical shell with parameters $L = 5R$, $k_{cyl,st} = k_{cyl,rings} = 10$, the critical pressure for external one-sided reinforcement exceeds that for two-sided one.

The results in Tables 1 and 2 correspond to the bifurcation modes of the compartments, making it possible to select the number of reinforcing ring stiffeners to achieve equal stability of the compound structure according to the forms of buckling. For internal reinforcement at $T^* = 0$ and $l_0 = 0.5l_1$, equal stability is achieved for the following configurations:

- $L = 2.39R$, with 10 stringers in each compartment, 5 ring stiffeners in the conical one and 18 in the cylindrical one;

- $L = 5R$, with 10 stringers, 3 ring stiffeners in the conical one and 90 in the cylindrical one.

For the first case, the critical pressure of global buckling of the compound "cone–cylinder" system (without connecting ring stiffeners) is $q^* = 2.5557$ Pa, which is about 3.8 times lower than the local critical pressure. For the second case, global buckling occurs at $q^* = 5.4834$ Pa, about 1.36 times lower than the local value. Among these, the structure with the smaller length parameter is more stable. The second type of structure is characterized by a larger length parameter and a significantly greater number of stiffening elements compared to the first type. However, for the same number of stiffening elements, the critical pressure is $q^* = 2.0907$ Pa. Among the two types considered, the structure with the smaller length parameter exhibits higher stability.

The bifurcation modes of a "cone–cylinder" system with $L = 5R$, internally reinforced with 10 stringers in each compartment and 3 ring stiffeners in the conical one, were investigated. The influence of the number of intermediate ring stiffeners in the cylindrical compartment and the stiffness parameters of connecting ring

Table 1

Influence of the number and arrangement of stiffening ribs on the critical pressure parameter for the cylindrical compartment

$L = 2.39R$		Reinforcement					$L = 5R$		Reinforcement		
		internal		external		two-sided type 1			internal	external	two-sided type 1
$k_{cyl,st}$		10	20	10	20	10	$k_{cyl,st}$		10	10	10
Number of ring stiffeners	10	7.361	7.511	8.115	8.138	8.761	Number of ring stiffeners	10	2.236	2.509	2.507
	15	8.970	9.427	10.258	10.380	11.128		50	5.288	6.433	7.569
	17	9.504	9.966	10.949	11.077	12.074		80	6.965	8.522	11.355
	18	9.763	10.227	11.283	11.410	12.546		90	7.456	9.1221	12.615
	20	10.26	10.733	11.929	12.054	13.491		100	7.919	9.685	13.876

Table 2

Influence of the number of stiffening ribs on the critical pressure parameter q^* for the conical compartment

$l_0 = 0.5l_1$		Reinforcement								
		internal			external			two-sided type 1		two-sided type 2
$k_{cone,st}$		9	10	20	9	10	20	10	20	10
Number of ring stiffeners	3	7.486	7.525	7.921	8.169	8.186	8.24	8.204	8.545	8.089
	4	8.625	8.665	9.064	9.573	9.590	9.694	9.652	10.118	9.535
	5	9.716	9.756	10.158	10.916	10.933	11.128	11.085	11.552	10.965
	6	10.762	10.802	11.208	12.201	12.219	12.547	12.504	12.974	12.381
	7	11.766	11.807	12.217	13.434	13.452	13.952	13.909	14.38	13.782
	8	12.731	12.772	13.188	14.618	14.636	15.344	15.301	15.781	15.169

Table 3

Influence of reinforcement on the buckling characteristics of the "cone-cylinder" structure

	$G_1 = G_2 = 0$			$G_1 = 100$, $G_2 = 10$	$G_1 = 5{,}000$, $G_2 = 10$
$k_{cyl,rings}$	20	50	90	90	90
q^*	2.1258	3.9524	5.4834	7.7754	8.7749
n	3	3	3	6	3

stiffeners was analyzed. The corresponding critical parameters and bifurcation modes at $T^* = 0$ are presented in Table 3.

Under combined loading by external pressure with axial forces, Fig. 2 presents the boundary curves separating the stability region from the buckling region of the compound "cone–cylinder" shell system with connecting ring stiffeners characterized by stiffness parameters $G_1 = 5{,}000$ and $G_2 = 10$. The compound system is considered with the conical compartment having the parameter $l_0 = 0.5l_1$, while the cylindrical compartment has the length $L = 2.39R$ (Fig. 2, *a*) or $L = 5R$ (Fig. 2, *b*). Both compartments are reinforced with 10 stringers. The conical compartment contains 5 (Fig. 2, *a*) or 3 (Fig. 2, *b*) intermediate ring stiffeners, whereas the cylindrical compartment contains 10 or 18 (Fig. 2, *a*), and 18 or 90 (Fig. 2, *b*). The number of ring stiffeners is selected so that the compartments can be considered approximately equally stable. Solid lines correspond to the internal arrangement of stiffening ribs, dashed lines to the external arrangement, and dash-dotted lines to two-sided reinforcement.

Within the considered loading range, compressive axial force T^* reduces the critical external pressure, while tensile force increases it.

The numerical analysis showed that external placement of reinforcing load-carrying elements provides higher critical loads compared with internal placement and is therefore more efficient in terms of structural stability for the considered parameters.

Conclusions. An analytical-numerical approach and algorithms for applying computer algebra systems to derive governing differential stability equations for reinforced compound shell systems are proposed. The analysis is carried out under combined loading, taking into account the eccentricity of the arrangement of reinforcing load-carrying elements and the discrete distribution of ring stiffening ribs.

For shell structures of the "cone–cylinder" type, algorithms for the numerical solution using the finite difference method and for computer visualization of the bifurcation modes of individual compartments and the compound system are implemented in the Maple system. The dependence of critical loads on the stiffness parameters of the structure is investigated, as well as the interaction between local and global buckling modes under different configurations of reinforcing load-carrying elements.

A comparison of the obtained stability equations for the considered class of compound shell systems with known equations for particular cases is presented, taking into account the stiffness of ring stiffeners out of the plane of the initial curvature and their influence on the critical parameters.

The analysis shows the effectiveness of external placement of reinforcing load-carrying elements for given geometric and stiffness characteristics of the reinforced shell structure. The possibility of designing structures with equal stability of compartments and spans with respect to local and global bifurcation modes is established by varying the number of ring stiffeners in the cylindrical compartment. Based on the proposed approach, boundary curves separating the stability regions of the considered structure under two-parameter combined loading with dominant external pressure are constructed.

Further research should focus on the effect of inversion of the influence of the eccentricity of the reinforcing load-carrying system in a compound shell system. From the standpoint of load-bearing capacity, an important factor is the shape of the limiting surface separating the stability domain under multiparameter com-

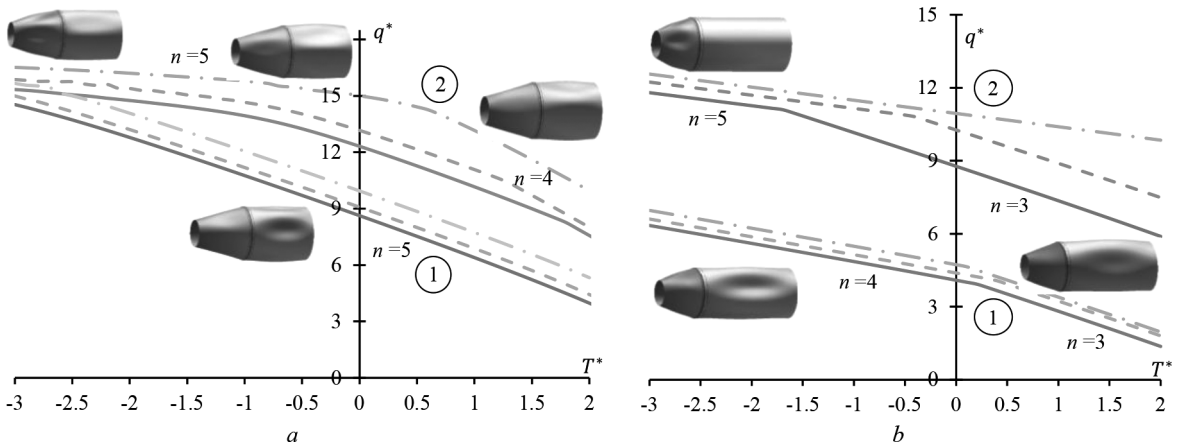

Fig. 2. Boundary curves of stability for the reinforced compound shell system "cone-cylinder" with connecting ring stiffeners

bined loading, taking into account boundary conditions. This makes it possible to visualize and quantitatively assess the safety and reliability of the structure under operating conditions.

References.

1. Dehtyarev, O. V., Grystchak, V. Z., & Sirenko, V. M. (Eds.) (2020). *Mathematical Models and Prediction of Damage Loads in Rocket-Space Systems*: *collective monograph*. Zaporizhzhia: Vydavnychyi dim "Helvetyka". ISBN 978-966-992-583-1.

2. Degtyarev, M. A., Shapoval, A. V., Gusev, V. V., Avramov, K. V., & Sirenko, V. N. (2019). Structural optimization of waffle shell sections in launch vehicles. *Strength of Materials*, *51*(2), 223-230. https://doi.org/10.1007/s11223-019-00068-7

3. Bai, X., Xu, W., Ren, H., & Li, J. (2017). Analysis of the influence of stiffness reduction on the load carrying capacity of ring-stiffened cylindrical shell. *Ocean Engineering*, *135*, 52-62. https://doi.org/10.1016/j.oceaneng.2017.02.034

4. Ifayefunmi, O., & Ruan, D. (2022). Buckling of Stiffened Cone-Cylinder Structures Under Axial Compression. *International Journal of Applied Mechanics*, *14*(7), 2250075. https://doi.org/10.1142/S1758825122500752

5. Cao, X., Wang, L., Li, Z., Zhang, H., & Wang, X. (2022). An analytical approach to global buckling of ring-stiffened sandwich cylindrical shells. *Frontiers in Materials*, *9*, 1064695. https://doi.org/10.3389/fmats.2022.1064695

6. Gristchak, V. Z., Hryshchak, D. V., Dyachenko, N. M., Sanin, A. F., & Sukhyy, K. M. (2023). Bifurcation state and rational design of three-layer reinforced compound cone-cylinder shell structure under combined loading. *Space Science and Technology*, *29*(6), 26-41. https://doi.org/10.15407/knit2023.06.026

7. Yang, Z., Zhang, X., Pan, G., & Xu, Y. (2023). Buckling and strength failure for unstiffened and ring-stiffened composite shells. *Ocean Engineering, 278*, 114513. https://doi.org/10.1016/j.oceaneng.2023.114513

8. Shen, K.-C., Jiang, L.-L., Yang, Z.-Q., & Pan, G. (2022). Buckling of a composite cylindrical shell with cantilever-like boundary conditions under hydrostatic pressure. *Journal of Marine Science and Engineering*, *10*(2), 126. https://doi.org/10.3390/jmse10020126

9. Gristchak, V., Hryshchak, D., Dyachenko, N., & Degtiarenko, P. (2020). Stability and rational design of the "barrel–ogive" type strengthened shell structures under combined loading. *Eastern-European Journal of Enterprise Technologies*, *4/7*(106), 6-15. https://doi.org/10.15587/1729-4061.2020.209228

10. Xu, Y., Tong, Y., Liu, M., & Bajracharya, S. (2016). A new effective smeared stiffener method for global buckling analysis of grid stiffened composite panels. *Composite Structures, 158*, 83-91. https://doi.org/10.1016/j.compstruct.2016.09.015

11. Pasternak, H., Li, Z., Juozapaitis, A., & Daniūnas, A. (2022). Ring Stiffened Cylindrical Shell Structures. *Applied Sciences*, *12*(22), 11665. https://doi.org/10.3390/app122211665

12. Khalili, F., & Showkati, H. (2012). T-ring stiffened cone-cylinder intersection under internal pressure. *Thin-Walled Structures*, *54*, 54-64. https://doi.org/10.1016/j.tws.2012.01.015

13. Gristchak, V. Z., Hryshchak, D. V., Dyachenko, N. M., & Kuprikov, V. O. (2024). Bifurcation States and Visualization of Postcritical Deformation of Three-Layer Composite Structures. *Computer Science and Applied Mathematics*, *2*, 39-53. https://doi.org/10.26661/2786-6254-2024-2-05

14. Hryshchak, D. V. (2020). *Computer algebra in solving applied problems of structural mechanics with variable parameters*. Vydavnychyi dim "Helvetyka". ISBN N978-966-992-422-3.

15. Gontarovskyi, P. P., Smetankina, N. V., Garmash, N. G., Melezhyk, I. I., & Protasova, T. V. (2024). Assessment of Stress–Strain State of Lightweight Shell of Waffle Fuel Tank of Launch Vehicle. *International Applied Mechanics*, *60*, 454-463. https://doi.org/10.1007/s10778-024-01297-3

16. Gontarovskyi, P. P., Smetankina, N. V., Garmash, N. G., Melezhyk, I. I., & Protasova, T. V. (2023). Three-Dimensional Stress–Strain State Analysis of the Bimetallic Launch Vehicle Propellant Tank Shell. *Strength of Materials*, *55*, 916-926. https://doi.org/10.1007/s11223-023-00582-9

17. Chernobryvko, M. V., Avramov, K. V., Romanenko, V. N., Batutina, T. J., & Suleimenov, U. S. (2016). Dynamic instability of ring-stiffened conical thin-walled rocket fairing in supersonic gas stream. *Journal of Mechanical Engineering Science*, *230*(1), 55-68. https://doi.org/10.1177/0954406215592171

18. Ismail, M. S., Mahmud, J., Ifayefunmi, O., & Purbolaksono, J. (2025). A Comprehensive Review of Curved Shell Structures Against Buckling Failures. *Preprints*, 2025030443. https://doi.org/10.20944/preprints202503.0443.v1

19. Krivenko, O. P., Lizunov, P. P., & Kalashnikov, O. B. (2024). The influence of geometrical shape on the stability of thin-walled axisymmetric shells. *Upravlinnia rozvytkom skladnykh system (Management of Development of Complex Systems)*, (57), 102-106. https://doi.org/10.32347/2412-9933.2024.57.102-106

20. Yegorov, Y., & Kucherenko, O. (2023). Computer modelling of thin-walled shell structures with geometric imperfections. *Strength of Materials and Theory of Structures*, *111*, 205-213. https://doi.org/10.32347/2410-2547.2023.111.205-213

21. Zhu, Y., Guan, W., Wang, W., Dong, C., & Zhang, J. (2023). Buckling performance of stiffened polymer composite cylindrical shell. *Engineering Structures, 295*, 116848. https://doi.org/10.1016/j.engstruct.2023.116848

22. Xiang, Y., Yin, Y., Jing, X., Li, X., Jin, H., & Zhang, D. (2025). Buckling Strength and Sealing Performance of External Pressure-Resistant Stiffened Cylindrical Shell Structures with Split-Structure Characteristics. *Aerospace, 12*(11), 1018. https://doi.org/10.3390/aerospace12111018

23. Wang, B., Tian, K., Hao, P., Zheng, Y., Ma, Y., & Wang, J. (2016). Numerical-based smeared stiffener method for global buckling analysis of grid-stiffened composite cylindrical shells. *Composite Structures, 152*, 807-815. https://doi.org/10.1016/j.compstruct.2016.05.096

24. Th. von Kármán & H. L. Dryden (Eds.). (2013). *Theory of Elastic Thin Shells*. Elsevier. ISBN: 978-0-08-009561-5.

25. Tănase, M., & Lvov, G. (2025). Analytical and numerical study of the buckling of steel cylindrical shells reinforced with internal and external FRP layers under axial compression. *Computer Modeling in Engineering & Sciences, 144*(1), 717-737. https://doi.org/10.32604/cmes.2025.067891

Стійкість і біфуркації ексцентрично підкріплених складених оболонкових конструкцій засобами комп'ютерної алгебри

Д. В. Грищак[1], *В. З. Грищак*[*2], *Н. М. Д'яченко*[3], *В. О. Купріков*[3]

1 – Конструкторське бюро «Південне» імені М. К. Янгеля, м. Дніпро, Україна

2 – Національний технічний університет "Дніпровська політехніка, м. Дніпро, Україна

3 – Запорізький національний університет, м. Запоріжжя, Україна

[*] Автор-кореспондент e-mail: HRYSHCHAK.V.Z@mnu.one

Мета. Створення аналітико-чисельного підходу й алгоритмів застосування системи комп'ютерної алгебри (СКА) для аналізу впливу характеру розташування підкріплюючих силових елементів на стійкість складених ортогонально підкріплених оболонкових конструкцій при комбінованому зовнішньому навантаженні. Досягнення мети передбачає отримання розв'язувальних рівнянь, створення алгоритмів дослідження залежності критичних зусиль від геометричних і жорсткісних параметрів відсіків, розташування підкріплюючого силового набору й характеру зовнішнього навантаження.

Методика. Запропонована методика отримання основних рівнянь із застосуванням системи Maple й алгоритм числового розв'язання задачі стійкості методом скінченних різниць із комп'ютерною візуалізацією форм біфуркації відсіків і складеної оболонкової системи.

Результати. На базі СКА запропоновано підхід до розв'язання задачі стійкості складеної підкрі-

пленої оболонкової системи «конус–циліндр» при комбінованому зовнішньому навантаженні й наявності особливостей жорсткісних параметрів відсіків. Запропоновані алгоритми дослідження впливу ексцентриситету силового набору й дискретності розташування шпангоутів на критичні навантаження та форми біфуркації конструкції. Розроблено алгоритм комп'ютерної візуалізації процесів втрати стійкості з отриманням характерних форм біфуркації й побудовою граничних кривих, що відокремлюють область стійкості досліджуваної конструкції за умови превалюючого впливу зовнішнього тиску.

Наукова новизна. Встановлено вплив ексцентриситету підкріплюючих силових елементів відносно серединної поверхні на критичні навантаження та форми біфуркації складеної оболонкової конструкції при двопараметричному зовнішньому навантаженні осьовими стискаючими зусиллями й зовнішнім тиском. Виявлені особливості впливу жорсткісних характеристик силового набору на стійкість системи на базі запропонованого алгоритму автоматизованого виведення розв'язувальних диференціальних рівнянь із застосуванням систем комп'ютерної алгебри. Надані результати чисельного аналізу критичних зусиль системи типу «конус–циліндр».

Практична значимість. Проведений аналіз надає можливість виявити вплив характеру розташування та жорсткості підкріплюючих силових елементів на несучу здатність складених оболонкових систем типу «конус–циліндр». При цьому враховується взаємодія локальних і загальних форм біфуркації при комбінованому навантаженні. Застосування СКА дозволяє побудувати граничні криві, що відокремлюють область стійкості досліджуваної системи залежно від характеру розташування ребер жорсткості. Отримані результати дозволяють здійснювати проєктування конструкцій, раціональних із точки зору критичного стану.

Ключові слова: *комп'ютерна алгебра, оболонка, підкріплюючі елементи, ексцентриситет, рівняння стійкості, форми біфуркації*